

One might expect that the directivity, which is the ratio of the forward power to the backward power from the amplifier system, would be strongly influenced by the phase adjustment of the coupling circuit. But the experimental results showed that the phase adjustment effect was not significant. For example, the directivity of the direct coupled amplifier was 10 db, and on the other hand, the directivity of the phase shifter coupled amplifier was 11 db. The phase shifter setting for optimizing gain was different from the phase shifter setting for optimizing the directivity.

CONCLUSIONS

Adjusting the phase of the feedback between the amplifier stages of the cascaded 2K25 reflex klystron ampli-

fier is necessary if more than twice the gain in db of a single stage amplifier is to be obtained. The phase adjustment gives high gain and reasonably low noise figure, and, consequently, high sensitivity is obtained. The use of the phase shifter made the system somewhat narrow band but stable. The linearity and dynamic range of the cascaded amplifier were improved considerably using the phase adjustment, but the effect of the phase adjustment on the directivity was not significant.

ACKNOWLEDGMENT

The author wishes to thank Professor E. H. Scheibe, University of Wisconsin, for his valuable discussion, and Dr. J. D. Horgan, S. Krupnik, L. Heiting, and J. Tsui, Marquette University, for their assistance.

TE Modes of the Dielectric Loaded Trough Line*

MARVIN COHN†, MEMBER, IRE

Summary—The properties of TE modes on a dielectric loaded trough waveguide have been investigated. In the case of the dominant mode of this line (TE_{20}), families of design curves giving the field distribution, guide wavelength, power handling capability, wall losses, and dielectric losses as a function of operating wavelength, waveguide dimensions and dielectric constant are presented. For a loosely bound wave, the losses are comparable to those of conventional rectangular waveguide and the power handling capability is an order of magnitude greater. The apparatus and procedure used to measure guide wavelength, rate of field decay in the transverse direction, and attenuation are described. The measured performance is in close agreement with the theoretically predicted characteristics.

INTRODUCTION

THE transmission line to be investigated consists of a rectangular trough structure with a dielectric slab lying on the bottom. A cross section of this line and the coordinate system used in the analysis are shown in Fig. 1. The TE surface wave modes which can propagate in the dielectric loaded trough line have been previously determined in an analysis of the dielectric loaded parallel plane waveguide.¹ A transverse resonance approach has been used by Hatkin² to determine some of the characteristics of these TE modes on an infinite dielectric sheet. The dielectric loaded parallel

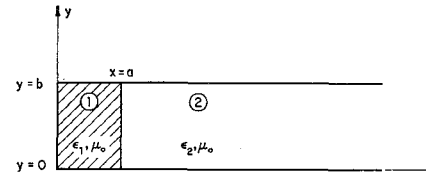


Fig. 1—Cross section of the dielectric loaded trough line. The positive z direction is out of the paper.

plane waveguide consists of two dielectric loaded trough waveguides lying back to back along the $x=0$ plane with the common conducting plate removed. The above mentioned analysis has shown that the dielectric loaded parallel plane waveguide can support a class of TE modes, whose field structure is similar to the TE modes of rectangular waveguide. These TE modes display either even or odd symmetry about the geometrical plane of symmetry ($x=0$). The even symmetry modes correspond to m being an odd integer and vice versa. It was further shown that if a conducting wall is placed at the $x=0$ plane, all of the even TE modes will be suppressed, but the odd modes will be unaffected. The dominant mode of the resulting trough line (half of the original line) will be the TE_{20} mode.

The purpose of this extension to the previous work is to present a series of design curves applicable to the trough line. It is recommended that the reader refer to the earlier work for a derivation of the properties of the odd symmetry TE modes.

A dielectric loaded trough line has been built and measurements have been made of the guide wavelength, rate of field decay in the transverse direction and at-

* Received by the PGM TT, February 8, 1960, revised manuscript received, April 21, 1960. This research was supported by the U. S. Air Force through the Wright Air Dev. Div., of the Air Res. and Dev. Command.

† Radiation Lab., The Johns Hopkins University, Baltimore, Md.

¹ M. Cohn, "Propagation in a dielectric-loaded parallel plane waveguide," IRE TRANS. ON MICROWAVE AND THEORY TECHNIQUES, vol. MTT-7, pp. 202-208; April, 1959.

² L. Hatkin, "Analysis of propagating modes in dielectric sheets," PROC. IRE, vol. 42, pp. 1565-1568; October, 1954.

tenuation in order to verify the theoretically predicted performance.

FIELD DISTRIBUTION

It has been previously shown,¹ that the fields of the trough line TE modes are sine or cosine functions of x in the dielectric region and decay exponentially in the air space according to $e^{k_{20}(a-x)}$. In the case of the dominant mode, the angle of sinusoidal or cosinusoidal variation is restricted to the second quadrant ($\pi/2 < k_{10}a < \pi$). Fig. 2 is a family of curves of $(k_{10}a)$ as a function of $(2a/\lambda_o)$ and the difference between the inner and outer dielectric constants (ΔK), where $\Delta K = K_1 - K_2 = \epsilon_1/\epsilon_o - \epsilon_2/\epsilon_o$. A similar family of curves for the outer transverse distribution parameter $(k_{20}a)$ is presented in Fig. 3. The field configuration of this mode is identical to that previously published¹ for the TE₂₀ mode of the parallel plane line.

POWER HANDLING CAPABILITY

If the field intensities are the same, the axial power flow of a TE mode on the trough line is equal to half of the axial power flow of the corresponding TE mode of the parallel plane line.

$$P_{zo} = \frac{|A_o|^2 \pi b a}{2} \sqrt{\frac{\mu_0}{\epsilon_0}} \left(\frac{2a}{\lambda_o} \right) \frac{\sqrt{\pi^2 K_1 \left(\frac{2a}{\lambda_o} \right)^2 - (k_{10}a)^2}}{2(k_{10}a)^2} \left[1 - \frac{\tan k_{10}a}{k_{10}a} \right]. \quad (1)$$

For the TE₂₀ mode, the maximum electric field is located in the dielectric at the transverse position where $k_{10}x = \pi/2$. As a safety factor, the breakdown power level P_{bd} will be calculated assuming that the maximum electric field E_{bd} which can exist is the breakdown field of air (despite the fact that this maximum field occurs in a dielectric loaded region). E_{bd} is taken as 15,000 volts per centimeter (a safety factor of approximately two) to conform to standard waveguide calculations. From the equation for E_{bd} , it is apparent that

$$|A_o| = \frac{k_{10}}{\omega \mu_0} |E_{bd}|. \quad (2)$$

If (2) is substituted into (1), the following equation for the breakdown power level of the TE₂₀ mode in the trough line is obtained:

$$\frac{P_{bd}}{ab} = \frac{4.755 \cdot 10^8}{(2a/\lambda_o)} \left[1 - \frac{\tan k_{10}a}{k_{10}a} \right] \cdot \sqrt{\pi^2 K_1 \left(\frac{2a}{\lambda_o} \right)^2 - (k_{10}a)^2}. \quad (3)$$

For the case where $K_2 = 1$, this function has been calculated for several values of $(2a/\lambda_o)$ and K_1 . The result-

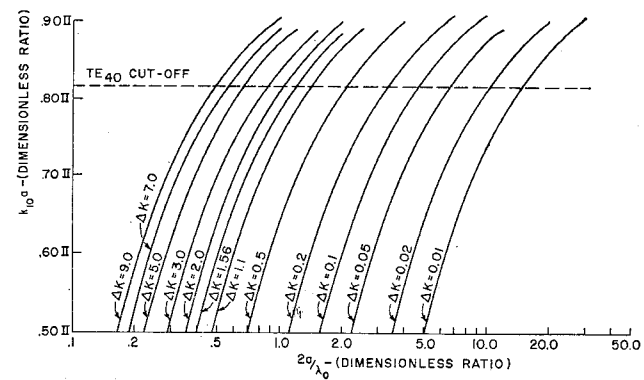


Fig. 2—Curves of the inner transverse distribution parameter ($k_{10}a$) of the TE₂₀ mode as a function of normalized slab width ($2a/\lambda_o$), and the difference of the dielectric constants (ΔK).

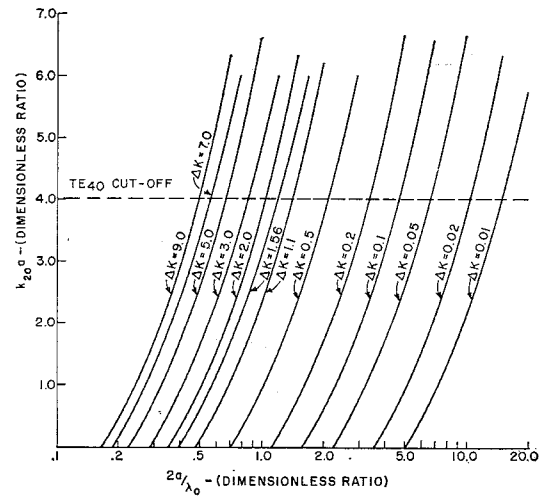


Fig. 3—Curves of the outer transverse distribution parameter ($k_{20}a$) of the TE₂₀ mode as a function of the normalized slab width ($2a/\lambda_o$) and the difference of the dielectric constants (ΔK).

ing family of curves is shown in Fig. 4. These curves show that when $(2a/\lambda_o)$ is only slightly greater than the critical magnitude required to sustain the TE₂₀ mode, P_{bd} becomes very large. This condition corresponds to a very loosely bound wave in which most of the energy is propagated in region 2 and the field extent in the x direction is very large. The TE₂₀ mode of the trough line is thus similar to the TE₁₀ mode of the dielectric loaded parallel plane line in that power levels an order of magnitude greater than those of conventional rectangular waveguide can be propagated if a sufficiently large structure (in the x direction) can be tolerated. The advantage is that single mode operation can be assured even with the larger guiding structure.

TRANSMISSION LOSSES

The attenuation due to losses in the dielectric (α_{do}) and in the parallel side walls (α_{wo}) of the trough guide is identical to that previously derived¹ for the parallel

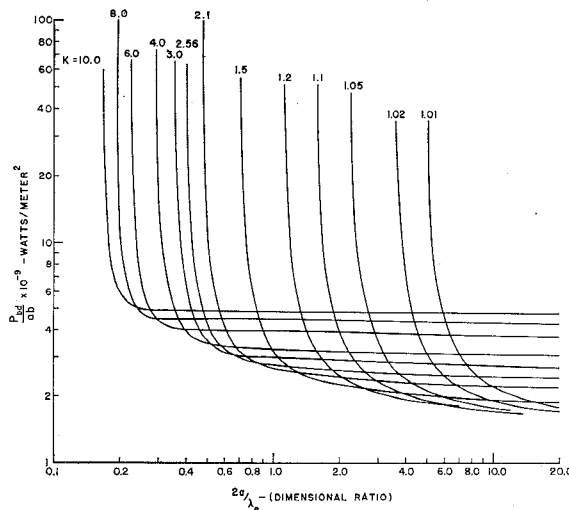


Fig. 4—Curves of the power handling capability (P_{bd}/ab) as a function of the normalized slab width ($2a/\lambda_o$) and dielectric constant (K_1). These curves are for the TE_{20} mode and the case where the outer region is air or vacuum.

plane waveguide and hence will not be repeated. For the TE_{20} mode and for $K_2=1$, a family of curves of the attenuation due to losses in the parallel side walls (α_{wo}) is presented in Fig. 5 for a range of ($2a/\lambda_o$) and many values of K_1 . The conductivity of copper ($\sigma_w=5.80\times 10^7$ mhos per meter) was used in this computation. The curves of Fig. 5 may be used for other wall materials if the values of attenuation obtained from them are multiplied by the square root of the relative resistance of the substituted material. Fig. 6 is a plot of the attenuation due to the dielectric loss ($\alpha_{do}\lambda_o$) as a function of ($2a/\lambda_o$) and many values of K_1 for the TE_{20} mode. These calculated results were plotted for a value of dielectric loss tangent $\phi_d=0.001$. These curves may be used for other values of ϕ_d if the values of α_{do} obtained are divided by 0.001 and multiplied by the loss tangent of the dielectric used.

In the case of the trough line, there is an additional component of attenuation due to the losses in the bottom plate (α_b) of the trough. The bottom plate wall loss per unit length in the z direction (P_b) is given by

$$P_b = \frac{1}{2} \sqrt{\frac{\omega\mu_o}{2\sigma_w}} \int_0^b |H_{z10}(x=0)|^2 dy \\ = \frac{b |A_{10}|^2}{2} \sqrt{\frac{\omega\mu_o}{2\sigma_w}}. \quad (4)$$

The attenuation per unit length due to the bottom plate loss is

$$\alpha_b = \frac{P_b}{2P_{zo}}. \quad (5)$$

If (1) and (4) are substituted into (5), the following equation for the attenuation due to the bottom plate loss is obtained:

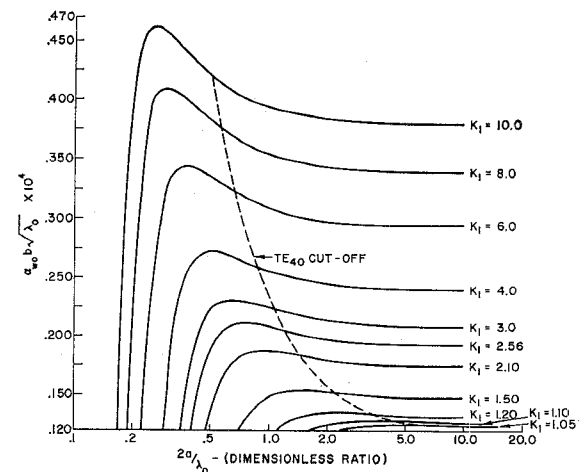


Fig. 5—Attenuation (in nepers per meter) due to the loss in the side walls as a function of the normalized slab width ($2a/\lambda_o$) and dielectric constant (K_1). These curves are for the TE_{20} mode and the case where the outer region is air or vacuum and the wall material is copper ($\sigma=5.80\times 10^7$ mhos per meter).

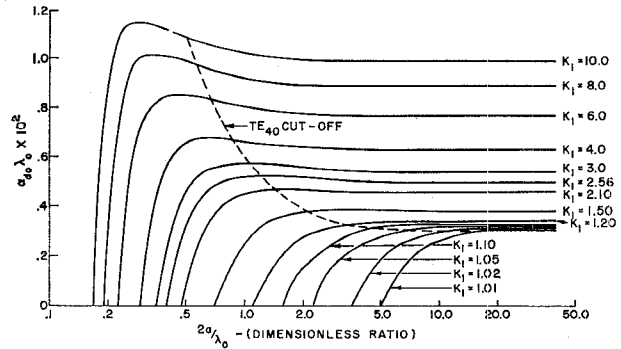


Fig. 6—Attenuation (in nepers per meter) due to the dielectric loss as a function of normalized slab width ($2a/\lambda_o$) and dielectric constant (K_1). These curves are for the TE_{20} mode and the case where the outer region is air or vacuum. The loss tangent (ϕ_d) equals 0.001.

$$\frac{\alpha_b a^2}{\sqrt{\lambda_o}} = \frac{0.01455}{\sqrt{\sigma_w}} \cdot \frac{(k_{10}a)^3}{\sqrt{\pi^2 K_1 \left(\frac{2a}{\lambda_o}\right)^2 - (k_{10}a)^2(k_{10}a - \tan k_{10}a)}}. \quad (6)$$

Assuming that material of comparable conductivity is used for the bottom plate as is used for the parallel side walls, the bottom plate component of attenuation is negligible compared to the side wall contribution.

MEASUREMENTS

The properties of the TE_{20} mode of the trough line have been measured in the line shown in Fig. 7. The view shown in Fig. 7 illustrates the method of constructing the line as well as the launching and collecting horns as one integral unit. The two parallel side walls of the trough are bolted firmly in place to make good electric

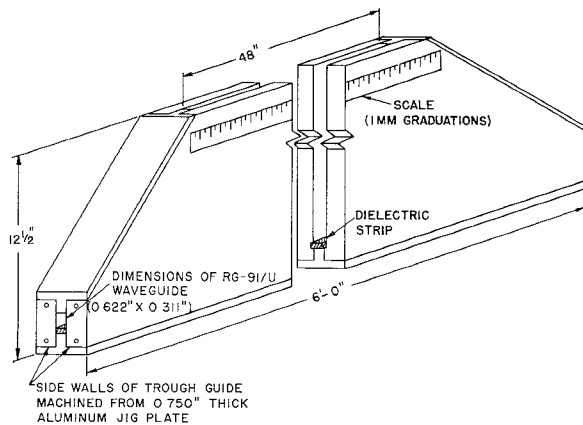


Fig. 7—Perspective view of the trough line.

contact. The spacing between these walls is maintained by the T shaped bars forming the bottom and sloping ends of the trough. Access to the inside of the line, to cement various dielectric strips in place, is easily achieved by removing one of the side walls. Fig. 8 shows a view of the inside of the trough line with one of the side walls removed. Also shown is one of the waveguide sections containing a length of dielectric tapered in the *H* plane. These sections provide a matched transition from the RG-91/U waveguide to the trough guide. The probe used for sampling the fields is also shown in this view. The probe is held in place by a carriage assembly which in turn slides along the top edges of the side walls of the trough. The vertical position of the probe can be changed by the rack and pinion arrangement shown. In order to insure accurate motion of the probe, the top edges of the side walls were carefully machined to be parallel to each other and to the inside of the bottom of the trough. Scales with one mm graduations and verniers were mounted on the probe and trough line so that the horizontal and vertical positions of the probe could be read to an accuracy of 0.1 mm.

The probe itself consists of Teflon filled RG-53/U waveguide (ID = 0.420 inch \times 0.170 inch) tapering to an inside dimension of 0.420 inch \times 0.006 inch at the tip. For many of the measurements it was desirable to have an even smaller aperture at the tip of the probe. In these cases silver paint was used to coat most of the opening, leaving an aperture of 0.125 inch \times 0.006 inch. A row of tapered resistance cards was mounted in front of the probe so that it appears to the impinging wave to be a matched load.

Two noncontacting short circuits were constructed. These also were held in carriages which slide on the top of the trough and whose horizontal position could be read to an accuracy of 0.1 mm. The shorts could be raised or lowered so that their lower ends were just above the top of the dielectric strip. When the dielectric strip is sufficiently thin relative to λ_0 , the rectangular waveguide formed by the length of dielectric under the short is beyond cutoff and, hence, very little energy leaks under the short.

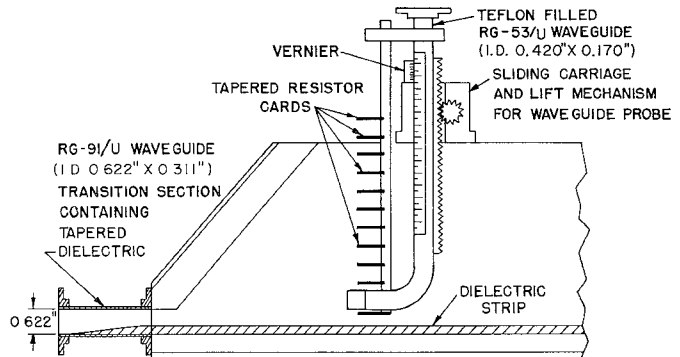


Fig. 8—Interior view of the trough line, with one side wall removed. A transition section, the probe assembly and its sliding carriage are shown.

In order to check the propagation characteristics of the TE_{20} mode of the trough line, it is necessary to determine the electrical properties of the dielectric strip independently of the trough line. The dielectric constant was measured in a rectangular waveguide using a standard short-circuited line method. The dielectric constant (K_1) was determined to be 2.60. The dielectric loss tangent (ϕ_d) was determined from measurements on a short-circuited polystyrene filled slotted line. Account was taken of the wall losses in the dielectric filled line and the dielectric loss and, hence, the dielectric loss tangent were determined from the measured decrease of VSWR with increasing distance from the short-circuited end. The average value of many measurements of loss tangent was 0.00052.

Two polystyrene strips whose thicknesses (a) were 0.399 cm and 0.638 cm were investigated. Their critical frequencies, which must be exceeded for the TE_{20} mode to propagate, were, respectively, 14.86 kmc and 9.30 kmc.

Regions of the trough line were found where the TE_{20} surface wave mode was undisturbed by radiation fields from the launching horn. A phase-sensitive bridge was set up and phase fronts were plotted in these regions and were observed to be parallel vertical planes which were properly spaced.

The waveguide wavelength (λ_0) was measured as a function of frequency in three different ways: 1) the probe and phase bridge were used to determine the spacing between successive phase fronts of equal phase; 2) a short circuit was used to set up a large reflection and the distance between nulls of the standing wave pattern was measured using the probe; and 3) two short circuits were used to set up a transmission cavity whose length could be varied. The cavity technique is described more thoroughly below in the discussion of attenuation measurements. The cavity technique gave the best results, since at resonance the surface wave fields are enhanced relative to the radiation fields. Fig. 9 shows that the measured values of λ_0 are in excellent agreement with the theoretically predicted values.

The rate of field decay in a transverse direction away from the dielectric-air interface was measured by a

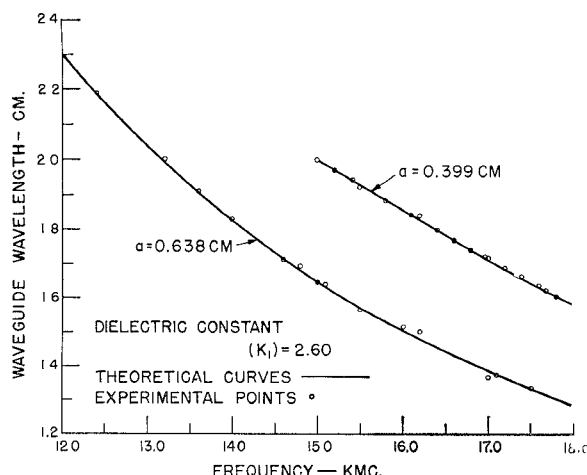


Fig. 9—Comparison of the measured and theoretical waveguide wavelength of the trough line TE_{20} mode as a function of frequency.

standard RF substitution method using the probe and a precision microwave attenuator. The experimental points and theoretical curves are shown in Fig. 10. Although individual points deviate from the theoretical curves, they follow the general direction of these curves very well. This measurement was most difficult to make in the extreme cases where the dielectric strip was either very thin (very loosely bound wave) or very thick (very tightly bound wave) compared to a wavelength. In the loosely bound case, the fields extend a large distance from the dielectric-air interface and as a result the field intensity at any point is low. In the tightly bound case, almost all of the energy propagates within the dielectric strip, but again the field intensity is very low in the air space. In each of these extreme cases, therefore, the stray radiation fields were comparable to the surface wave fields.

Measurements were made of the attenuation of this line using a variable length transmission cavity technique. This method, which has been previously discussed in the literature,³⁻⁵ is well-suited to attenuation measurements on a surface wave line. In the case of the trough line, the cavity was formed by two noncontacting shorts of the type described above. The short on the generator side was maintained in a fixed position, and the short on the detector side was adjusted to a resonant position as manifested by maximum output at the detector. The source klystron was swept in frequency causing the output waveform observed at the detector to be a replica of the cavity band-pass characteristic. The loaded Q of the cavity was determined from the three-db bandwidth of the cavity pass band character-

³ E. H. Scheibe, B. G. King, and D. L. Van Zeeland, "Loss measurements of surface wave transmission lines," *J. Appl. Phys.*, vol. 25, pp. 790-797; June, 1954.

⁴ S. P. Schlesinger and D. D. King, "Some Fundamental Properties of Dielectric Image Line," The Johns Hopkins University Radiation Laboratory, Baltimore, Md., Final Rept. AFCRC-TN-56-766, pp. 69-78; December, 1956.

⁵ D. D. King and S. P. Schlesinger, "Losses in dielectric image lines," *IRE TRANS. ON MICROWAVE THEORY AND TECHNIQUES*, vol. MTT-5, pp. 31-35; January, 1957.

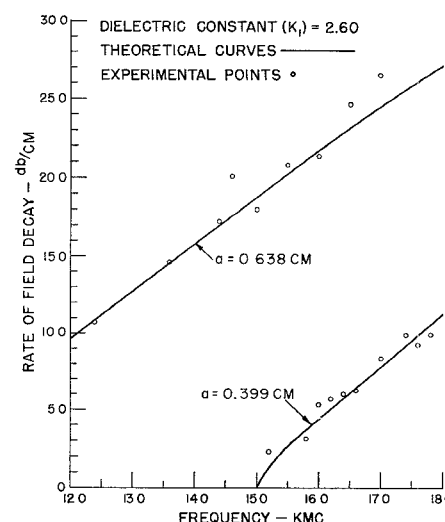


Fig. 10—Comparison of the measured and theoretical rate of field decay in the transverse direction for the trough line TE_{20} mode as a function of frequency.

istic. The short on the detector side was moved to another position where the output was maximized and again the loaded Q of the cavity was measured. The new short position is an integer number of half-waveguide wavelengths from its former position. This procedure was repeated for many short-circuit positions. From the manner in which the cavity Q varied with increasing cavity length, the attenuation per unit length of the trough guide could be determined.

The measured points and the theoretical curves of total attenuation as a function of frequency are shown in Fig. 11. The measured attenuation varies in the prescribed manner as a function of frequency; its magnitude, however, is somewhat higher than predicted. The discrepancy could be due to any or all of the following reasons:

- 1) The actual wall loss may be larger than theoretically predicted (as is invariably the case for rectangular waveguides), due to the roughness of the metal walls being comparable in magnitude to the depth of penetration of the RF currents.
- 2) The vinylite cement used to hold the dielectric strip in place has a considerably higher dielectric loss tangent than polystyrene.
- 3) Any irregularities along the line may cause radiation which would contribute to the total measured attenuation.

CONCLUSION

A number of families of curves have been presented which give the characteristics of the TE_{20} mode on a dielectric loaded trough line. If loosely bound, this mode, like the TE_{10} mode on the dielectric loaded parallel plane waveguide, has losses comparable to those of conventional rectangular waveguide and power handling capabilities an order of magnitude greater. The trough line has the advantages of being closed on three sides

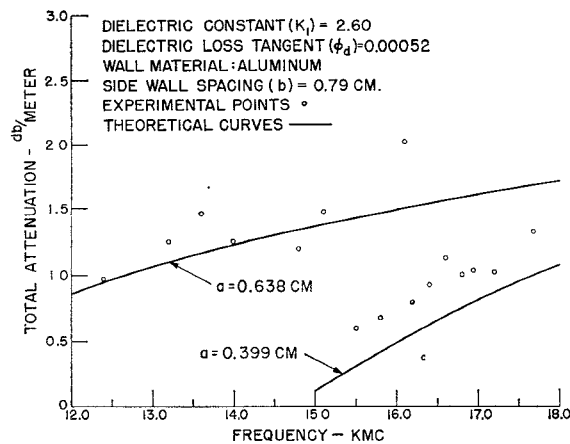


Fig. 11—Comparison of the measured and theoretical total attenuation of the trough line TE_{20} mode as a function of frequency.

and being smaller than the corresponding parallel plate line with comparable attenuation and power handling characteristics. The guide geometry and magnetic field configuration are appropriate for the fabrication of ferrite devices employing transverse magnetization.

The measurements of guide wavelength, rate of field decay and attenuation verify the theoretically predicted properties of this structure.

ACKNOWLEDGMENT

The author would like to thank Dr. E. S. Cassidy for his helpful discussions and criticisms, I. E. Pakulis for his careful carrying out of the measurements, Miss M. D. Velten for the numerical calculations and curve plotting, and J. W. Rodgers and W. Weber for construction of the trough line and associated apparatus.

Coupling of Modes in Uniform, Composite Waveguides*

L. C. BAHIANA† AND L. D. SMULLIN‡

Summary—The principle of coupling of modes is used to compute the phase constant in a uniform waveguide filled with two different dielectric materials. The natural modes of two hypothetical waveguides filled with the different dielectrics are computed. The propagation of the combined system is computed by considering the coupling between the two sets of modes. Comparison is made between the approximate theory and an exact theory.

I. INTRODUCTION

THE expression "uniform, composite waveguide" is used in this paper to describe any hollow metallic cylinder of arbitrary cross section filled with two or more homogeneous isotropic materials. Both the structure and the materials are uniform in the direction of propagation. Familiar examples of uniform, composite waveguides are waveguides partly filled with dielectric or magnetic material. The solution of the boundary value problem in such waveguides invariably leads to transcendental equations. Numerical solutions for a few particular cases have been published.¹

A different formulation of the problem is presented here and applied to the case of lossless waveguides containing two media. The fields are expressed in terms of the natural modes of two hypothetical waveguides, found by imposing short-circuit ($\bar{n} \times \bar{E} = 0$) or open-circuit ($\bar{n} \times \bar{H} = 0$) constraints at the boundary between the two media. Maxwell's equations are then transformed, by the use of conventional techniques, into an infinite set of coupled transmission-line equations. Although this formulation is completely general, its practical usefulness stems from the possibility of obtaining approximate solutions without cumbersome numerical computation.

II. FORMULATION OF THE PROBLEM

A. Equivalent Current Sheets

Fig. 1 shows the cross section of a composite waveguide. Surface S_1 is the metallic envelope. Surface S_2 is the boundary between the two media. The solution of Maxwell's equations in medium 1 is unique if either $\bar{n} \times \bar{E}$ or $\bar{n} \times \bar{H}$ is specified over the boundary. The same is true of medium 2. Let $\bar{n} \times \bar{E}_2(S_2)$, where \bar{E}_2 is the unknown field in region 2, be specified over S_2 . Then we can solve Maxwell's equations in medium 1. In order to do this, surface S_2 is replaced by a metallic wall S (short circuit, with $\bar{n} \times \bar{E} = 0$) and a magnetic current sheet $\bar{K}_m = \bar{n} \times \bar{E}_2(S_2)$. Mathematically, this is equivalent to

* Received by the PGM TT, January 20, 1960; revised manuscript received, April 14, 1960. This work was supported in part by the U. S. Army (Signal Corps), the U. S. Air Force (Office of Scientific Research, Air Research and Development Command), and the U. S. Navy (Office of Naval Research).

† Diretoria de Electrônica da Marinha, Ministério da Marinha, Rio de Janeiro, Brazil. Formerly with Mass. Inst. Tech., Cambridge, Mass.

‡ Dept of Electrical Engrg. and Res. Lab. of Electronics, Mass. Inst. Tech., Cambridge, Mass.

¹ T. Moreno, "Microwave Transmission Design Data," Dover Publications, Inc., New York, N. Y.; 1958.